

Nonlinear Pattern Formation in Active Optical Systems: Shocks, Domains of Tilted Waves, and Cross-Roll Patterns

K. Staliūnas,* G. Šlekys, and C. O. Weiss

Gr.4.3, Physikalisch Technische Bundesanstalt, 38116 Braunschweig, Germany

(Received 23 December 1996)

Vortices, shocks, domains of tilted waves, and cross-roll patterns are typical patterns of the complex Swift-Hohenberg equation, which describes spatiotemporal dynamics in nonlinear optical systems of large Fresnel number, such as lasers, optical parametric oscillators, and photorefractive oscillators. We show the occurrence of such “essentially nonlinear” patterns experimentally on a photorefractive oscillator and compare it with numerical solutions of the complex Swift-Hohenberg equation. [S0031-9007(97)04128-8]

PACS numbers: 42.65.Sf, 42.65.Yj

Lasers are generally known to emit radiation fields with simple spatial structure such as transverse resonator modes of low order. This simplicity is a consequence of the usual small Fresnel number of laser resonators. (The Fresnel number in optical systems corresponds to the aspect ratio of a conventional spatially extended nonlinear system.) On the other hand, it is known that lasers, or more generally resonators containing active or passive nonlinear media, are potentially capable of emitting fields with complicated structures of high spatial information content. This is seen from reduced laser equations in the form of the complex Ginzburg-Landau equation (CGLE) [1] or complex Swift-Hohenberg equation (CSHE) [2,3], which are the equation types at the basis of most pattern forming systems in Nature or physics.

Although complicated light field structures appeared in recent experiments with nonlinear optical systems [4,5], the patterns observed so far could be interpreted as the simultaneous excitation of transverse resonator modes. This implies that the patterns were dominated by boundary effects, rather than by the nonlinearity of the medium. “Essentially nonlinear” pattern formation of lasers, as it is described by the CSHE and CGLE, requires primarily a large Fresnel number of the resonator and, simultaneously, a high level of degeneracy of transverse mode families.

More complex patterns were reported in [6], where the Fresnel number was raised to hundreds—closer to the requirements for essentially nonlinear patterns. However, the complicated excitation geometry did not permit relation to a general nonlinear physics model in [6].

We show here experimentally that use of large Fresnel number resonators (few thousands) allow indeed essentially nonlinear pattern formation. We illustrate this by several structures typical for the CSHE, emitted by a photorefractive oscillator (PRO) which is equivalent to a class A laser [7]. Thus we conclude that nonlinear optics is, in reality and not only conceptually, capable of forming the full variety of complex structures typical for general pattern forming systems.

The CSHE is a universal order parameter equation describing pattern formation in the mean field approximation

in nonlinear optical systems, such as large Fresnel number class A lasers [2,3], PROs [7], and optical parametric oscillators [8]. It describes spatiotemporal dynamics of the order parameter $A(\vec{r}, t)$, which is proportional to the optical field envelope:

$$\partial_t A = pA + id(\Delta + \vec{\nabla}^2)A - \frac{(\Delta + \vec{\nabla}^2)^2}{\Delta\omega^2}A - A|A|^2. \quad (1)$$

For the case of a laser, p is the net gain parameter, Δ is resonator detuning, $d = L\lambda Q/(2\pi)$ is the diffraction coefficient, L is the total resonator length, λ is the wavelength, Q is the resonator finesse (photon lifetime in units of resonator round-trip time), and $\Delta\omega$ is the width of the gain line (or, equivalently, the mode linewidth for PROs). The transverse coordinates are scaled to the diameter of laser aperture, and the time t is scaled to the response time of the photorefractive medium (of order of seconds). For these scalings the diffraction coefficient is related to the Fresnel number of the resonator: $d = 1/F$. The CSHE (1) becomes the well-known CGLE for negative detunings; for positive detunings the CSHE displays patterns qualitatively different from the CGLE.

In the limit of zero (or negative) resonator detuning Δ in (1), the waves with zero transverse wave-number components are most strongly amplified: The Poynting vectors of radiation emitted are directed parallel to the optical axis of the resonator. For positive detuning, the Turing structures with nonzero transverse wave-number components are most favored. These correspond to a resonant ring in the spatial Fourier domain (the far field plane) with a radius dependent on detuning: $|k_\perp|^2 = \Delta$, and a width proportional to the gain line width $\Delta\omega$. The Poynting vectors are correspondingly tilted with respect to the optical axis.

One of the characteristic patterns of (1) for zero or negative detuning are vortices or spiral waves separated by “shocks.” Such patterns were studied numerically for the CGLE [1,9], and were observed experimentally in chemical and biological pattern-forming systems [10]. The shocks result from counterpropagating energy flows, which are generated by neighboring vortices [9]. This

energy flow in lasers originates from the variation of saturation along the radial direction inside a vortex.

For positive detuning, the most characteristic patterns of (1) are tilted waves, if no lateral boundaries are present. In this case, only one transverse wave number from the resonant ring wins in the nonlinear competition, and determines the pattern. In reality, the tilted waves can be influenced by lateral boundaries, which leads to domains of differently oriented tilted waves. Such tilted wave domains have been observed, among others, in two-component fluid systems [11]. They have also been theoretically predicted in class A lasers with sufficiently broad aperture [3].

The other characteristic pattern of the CSHE is the so-called “cross-roll pattern” [12]. This pattern (in the form of a square or rhombic “vortex lattice”) has been predicted for broad aperture lasers [3,13]. This cross-roll pattern appears as a superposition of two pairs of countertilted waves. As shown in Ref. [3], the square or rhombic vortex lattice is a pattern corresponding to a local minimum of the potential of the system, while the tilted wave corresponds to the global, deeper minimum.

Since class A lasers (and PROs) are described by (1), they should display the patterns discussed above. However, to our knowledge, experimental observations of such essentially nonlinear patterns in optical systems have not been reported. There are two main requirements for a laser to emit these patterns: (1) high level degeneracy of transverse (Gauss-Laguerre or Gauss-Hermite) modes, (2) a sufficiently large Fresnel number of the resonator. The Fresnel number determines the smallest spatial scale of the pattern: $x_{\min} = F^{-1/2}$ if the transverse coordinate is normalized to the width of the aperture. Our numerical calculations show that Fresnel number values sufficient for observation of the essentially nonlinear structures are $F > 10^3$ ($d < 10^{-3}$). (For smaller Fresnel numbers, boundaries play a significant role, and the essentially nonlinear structures such as domains of tilted waves, shocks, etc., are not sufficiently pronounced.) Typical resonator parameters ($L = 1$ m, $\lambda = 0.5 \times 10^{-6}$ m, $Q = 5$) and the requirement of a large Fresnel number ($F > 10^3$) lead to a diameter of aperture $x_{\text{aper}} > 20$ mm. This shows that to observe essentially nonlinear patterns the aperture of a plane resonator must be quite large, which probably explains the lack of corresponding observations so far.

In the experiments we exploited the fact that confocal resonators lead to the degeneracy of transverse modes (transverse mode continuum) and, apart from their central symmetry properties, correspond to plane resonators with an infinitely large Fresnel number. In other words, an exactly confocal resonator is completely diffractionless [$d = 0$ for (1)]. The importance of confocal resonators (and, more generally, of self-imaging ones) has been pointed out in [14] for (linear) image processing. Here we exploit the diffractionless confocal resonators in order to obtain a sufficiently large Fresnel number in our nonlinear system.

The analysis of near-confocal resonators (based, e.g., on a propagation matrix approach) yields the fact that,

if the displacement from the confocal resonator length l is small compared with the full resonator length L , then the order parameter equation (1), derived for a plane resonator, is also valid for a near-confocal one, but with a diffraction coefficient: $d = l\lambda Q/(2\pi)$. The pattern nearly reproduces itself in two resonator round-trips for near-confocal resonators. This imposes the central symmetry of the patterns. (For perfectly confocal resonators $l = 0$, and the dispersion and diffraction of the resonator vanish.)

We took these symmetry restrictions into account by integrating numerically in one-half of the integration region, and setting the order parameter in the other half of the region according to the symmetry conditions in every integration step. We used the split-step scheme on a spatial grid of (128×128) , with time step $\Delta t = 0.02$. For more details of the numerical scheme, see, e.g., Ref. [7]. The initial condition for the numerical integration was a randomly distributed field (Gaussian, δ correlated in space, noise). The equation was integrated in a unit size square region limited by zero boundaries corresponding to the cross section of the photorefractive crystal.

For experiments we used a photorefractive oscillator with BaTiO₃ as the active medium. The linear confocal resonator consisted of two highly reflecting mirrors with a radius of curvature of 350 mm. The crystal of $4.3 \times 4.3 \times 4.6$ mm dimensions was located close to one mirror and homogeneously illuminated by a single frequency Ar⁺ laser at 514 nm wavelength. The typical pump intensity was 20 mW/cm². We used the reflection from a crystal surface to outcouple radiation from the resonator. The difference l from the confocal length was about 5 mm, which corresponds to the Fresnel number of an equivalent plane resonator 5×10^3 .

Two characteristic planes were chosen for observation of the patterns within the cavity: (1) the crystal plane at the focus, which corresponds to the near field, and (2) the far mirror plane, which corresponds to the far field. The patterns were controlled by an intracavity circular aperture in the far field plane. Both planes were simultaneously imaged onto a charge-coupled device camera for recording.

For a totally open aperture, we observe in the near field a random small scale structure, as it is typically observed

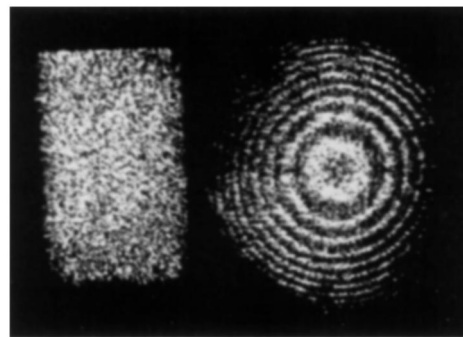


FIG. 1. Transverse pattern (near field, left; far field, right) as recorded experimentally on a PRO with a nearly confocal resonator. The intracavity aperture is completely open.

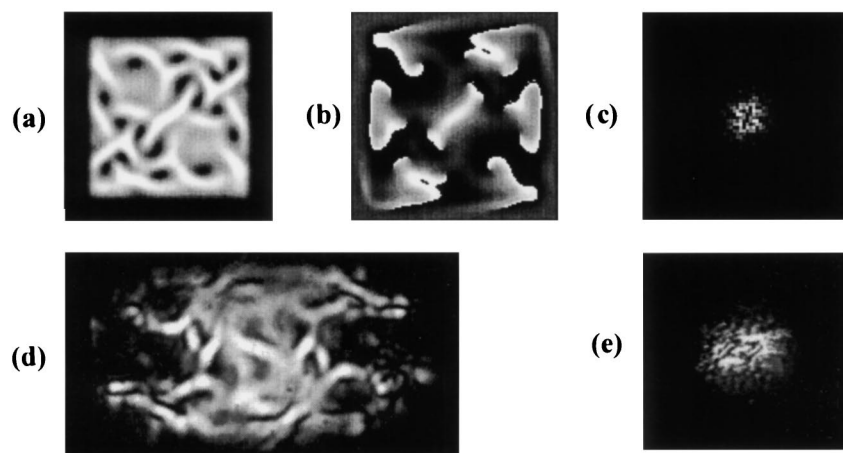


FIG. 2. Vortices separated by shocks. Numerically [(a)–(c)] and experimentally [(d)–(e)] obtained field distribution for zero detuning: near field amplitude (a), phase (b), far field amplitude (c). (d) and (e) are experimental images of the near field and far field plane. In the experiment, the resonator length is tuned so that the ring in the far field (e) contracts to a spot. The higher order rings (from Fig. 1) were removed by an intracavity aperture. The parameters for numerical integration are $p = 2.75$, $\Delta = 0$, $d = 10^{-3}$, $g = 5 \times 10^{-5}$. Pump field intensity in the experiment was two times above threshold.

in large Fresnel number photorefractive oscillators, and a set of concentric rings in the far field (Fig. 1). The rings in the far field indicate the slight deviation from confocality and are comparable with the rings observed in plane Fabry Perot resonators (e.g., as shown in [6]). Different rings correspond to different longitudinal orders of the resonant spatial wave vectors (or different longitudinal modes). A change of the resonator length leads to a change of the tilt angles of resonant wave vectors and the change of ring diameters in the far field.

To realize the single-longitudinal (but multitransversal) mode case described by CSHE, the emission was restricted to a single ring in the far field by the aperture in the far field plane. Under these conditions, the PRO displayed the typical patterns, predicted by (1), dependent on the resonator tuning.

Figures 2(a)–2(c) show a pattern calculated by the numerical integration of (1) for zero detuning and the experimentally recorded pattern (d) obtained by tuning the resonator length so that the ring in the far field contracted to a central spot (e). Optical vortices separated by shocks are seen in the near field patterns, both experimentally and numerically. The orientation of the shock boundaries and location of vortices was freely evolving in time and was not imposed by the boundaries of the system. The patterns display central symmetry, which is imposed by the confocality of the resonator.

Figure 3 shows domains of tilted waves obtained numerically from (1) for positive detuning [Figs. 3(a)–3(c)] and also experimentally [3(d)], with the resonator length tuned so that tilted components appear in the far field [3(e)]. The direction of the waves traveling inside the

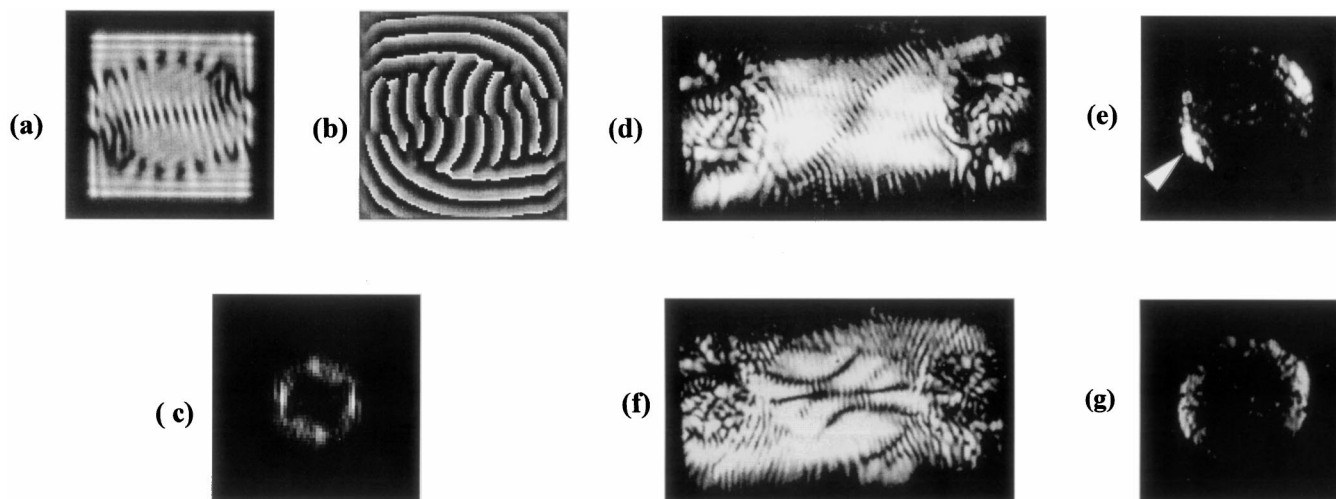


FIG. 3. Domains of tilted waves separated by a row of vortices. Numerically [(a)–(c)] and experimentally [(d)–(g)] obtained patterns for positive detuning. The resonator length was tuned to maintain the ring in the far field. The parameters for numerical integration are $p = 2.5$, $\Delta = 6$; other parameters in numerics and experiment are the same as in Fig. 2. Note the row of vortices separating the two domains of tilt in (d). Four domains of different tilts are visible in (f).

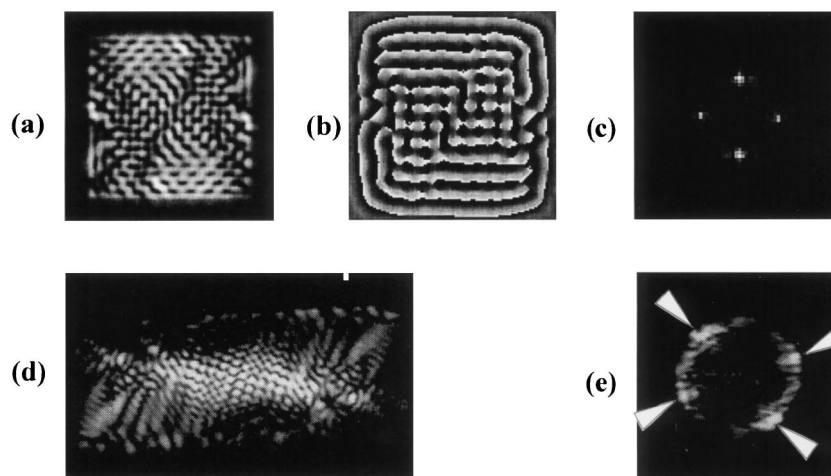


FIG. 4. The cross-roll pattern or square vortex lattice: numerically [(a)–(c)] and experimentally [(d) and (e)] obtained distributions for positive detuning. Everything is the same as Fig. 3, except for pump values. Numerically: $p = 1.5$; pump intensity in experiment was about 50% above threshold. Far field components in (e) are marked by arrows.

domains corresponds to the direction of the phase gradients, which can be seen from the phase picture in 3(b). The domains are separated by vortex rows as expected for domains of different flow. Experimentally, multiple domains were also recorded [3(f)]. The direction of the tilted waves in the domains can also be seen from the spot orientations on the far field ring (e.g., the orientation of the spots was freely changing in time, indicating that the orientation of the domains is independent of the boundaries, both in experiment and numerics).

The special case of four pairwise countertilted waves resulting in the cross-roll pattern is shown in Fig. 4. Numerically [Figs. 4(a)–4(c)] and experimentally [Figs. 4(d) and 4(e)] the cross-roll patterns appear at smaller pump parameters than the domains of tilted waves. Although the formation of the cross-roll pattern is intrinsic to the nonlinear system [3], the orientation of the counterpropagating tilted waves is influenced by boundaries. We performed numerical calculations using periodic boundary conditions (other parameters identical to those used for obtaining Fig. 4), where arbitrarily oriented cross-roll patterns were equally probable, which proves that the nonlinearity, and not the boundaries, is the primary mechanism for the formation of this pattern.

All experimentally and numerically observed patterns are dynamic. The temporal evolution occurs on a time scale given by the response time of the photorefractive material. Small resonator length drifts were, however, present in experiments, which could perhaps destabilize patterns. Consequently, from experimental observations alone, we cannot be completely sure of the intrinsic character of the dynamics of the patterns. However, the corresponding perturbation-free numerical calculations clearly showed self-sustained dynamics persisting longer than transients.

In conclusion, we have demonstrated for the first time an essentially nonlinear transverse pattern formation in an active nonlinear optical system (photorefractive oscillator) operating on a single longitudinal mode. These patterns, as

also obtained numerically from the order parameter equation (1) are (i) isolated vortices separated by shocks, (ii) domains of differently directed tilted waves, and (iii) cross-roll patterns. The requirement of high transverse mode degeneracy and a large Fresnel number was fulfilled using a confocal resonator, which, apart from its symmetry constraints, is equivalent to a plane resonator of a very high Fresnel number.

This work was supported by Deutsche Forschungsgemeinschaft and Volkswagen Stiftung.

*Electronic address: Kestutis.Staliunas@PTB.DE

- [1] P. Couillet, L. Gil, and F. Rocca, *Opt. Commun.* **73**, 403 (1989).
- [2] K. Staliunas, *Phys. Rev. A* **48**, 4847 (1993).
- [3] K. Staliunas and C. O. Weiss, *Physica (Amsterdam)* **81D**, 79 (1995).
- [4] F. T. Arecchi, G. Giacomelli, P. L. Ramazza, and S. Residori, *Phys. Rev. Lett.* **67**, 3749 (1991).
- [5] D. Dangoisse, D. Hennequin, C. Lepers, E. Louvergneaux, and P. Glorieux, *Phys. Rev. A* **46**, 5955 (1992).
- [6] A. V. Mamaev and M. Saffman, *Opt. Commun.* **128**, 281 (1996).
- [7] K. Staliunas, M. F. H. Tarroja, G. Sleky, C. O. Weiss, and L. Dambly, *Phys. Rev. A* **51**, 4140 (1995).
- [8] S. Longhi and A. Geraci, *Phys. Rev. A* **54**, 4581 (1996).
- [9] L. N. Howard and N. Kopell, *Stud. Appl. Math.* **56**, 95 (1977); I. S. Aranson, L. Kramer, and A. Weber, *Phys. Rev. E* **48**, R9 (1993).
- [10] Q. Ouyang and H. L. Swinney, *Chaos* **1**, 4 (1991), and references therein.
- [11] A. La Porta and C. M. Surko, *Phys. Rev. E* **53**, 5916 (1996).
- [12] M. Silber, H. Riecke, and L. Kramer, *Physica (Amsterdam)* **61D**, 260 (1992).
- [13] Q. Feng, J. V. Moloney, and A. C. Newell, *Phys. Rev. A* **50**, R3601 (1994).
- [14] J. A. Arnaud, *Appl. Opt.* **8**, 189 (1969).